Electronic Supplementary Information

Impact of Microstructure on the Electron-hole Interaction in Metal Halide Perovskites

Arman Mahboubi Soufiani[1†], Zhuo Yang[2†], Trevor Young[1], Atsuhiko Miyata[2], Alessandro Surrente[2], Alexander Pascoe[3], Krzysztof Galkowski[2,4], Mojtaba Abdi-Jalebi[5], Roberto Brenes[6], Joanna Urban[2], Nan Zhang[2], Vladimir Bulović[5], Oliver Portugall[2], Yi-Bing Cheng[3], Robin J. Nicholas[7], Anita Ho-Baillie[1*], Martin A. Green[1], Paulina Plochocka[2*], Samuel D. Stranks[5,6*]

[1]Australian Centre for Advanced Photovoltaics,
School of Photovoltaic and Renewable Energy Engineering,
University of New South Wales, Sydney, NSW 2052, Australia

[2]Laboratoire National des Champs Magnétiques Intenses, CNRS-UGA-UPS-INSA, 143 Avenue de Rangueil, 31400 Toulouse, France

[3]Department of Materials Science and Engineering, Monash University, Clayton, Vic 3800, Australia

[4]Institute of Experimental Physics, University of Warsaw - Pasteura 5, 02-093 Warsaw, Poland

[5]Cavendish Laboratory, University of Cambridge, J. J. Thomson Avenue, Cambridge CB3 0HE, United Kingdom

[6]Research Laboratory of Electronics, Massachusetts Institute of Technology, Cambridge, MA 02139, United States

[7]Clarendon Laboratory, University of Oxford, Parks Road, Oxford OX1 3PU, United Kingdom

[†] These authors contributed equally to this work.

[*]e-mail:
sds65@cam.ac.uk
paulina.plochocka@lncmi.cnrs.fr
a.ho-baillie@unsw.edu.au

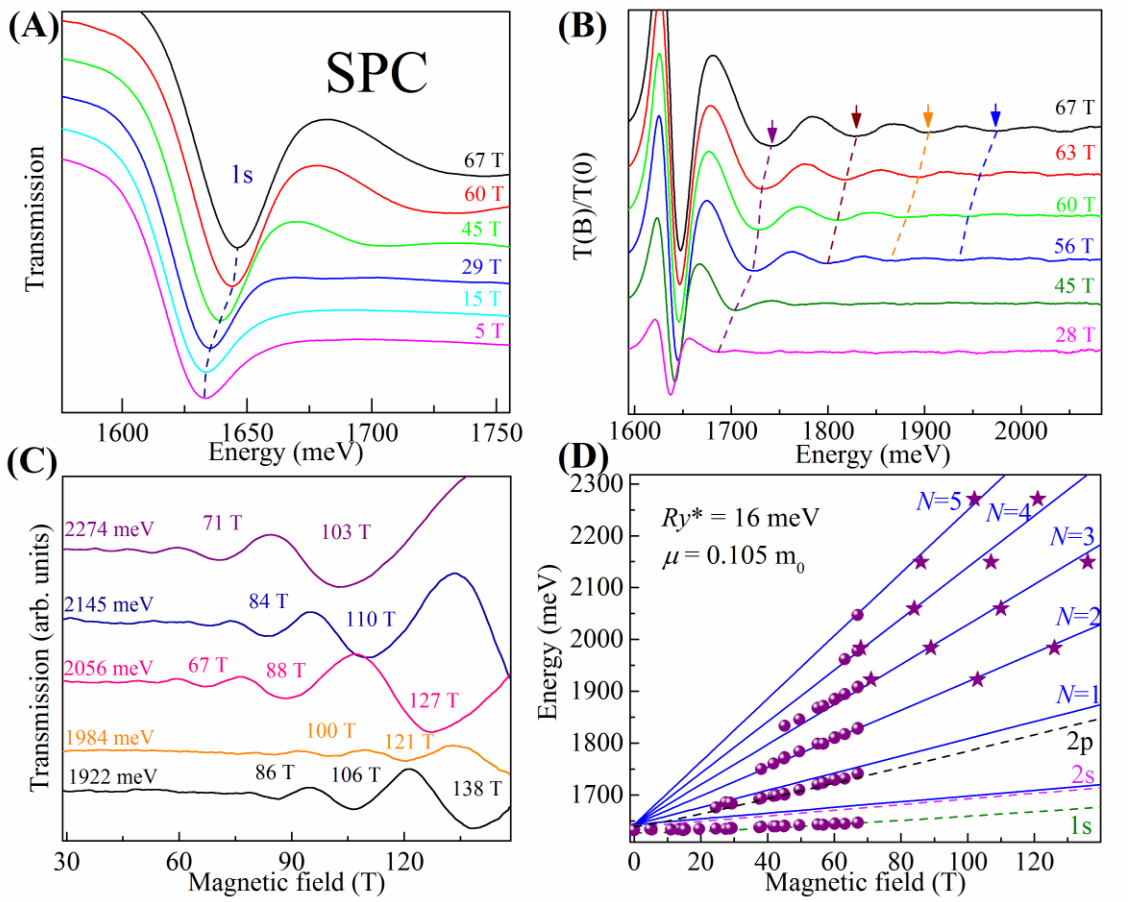

Figure S1 Magneto-optical transmission spectrum and fan chart measured at 2 K. A) Sequence of typical optical transmission spectra of the **SPC** sample measured at the indicated magnetic fields which show the 1s excitonic transition with increased transmission. **B)** Sequences of the ratios of the transmission spectra in magnetic field $T(B)$ to that measured at zero field $T(0)$. The resonant absorption features of the free carrier Landau levels correspond to minima. **C)** Typical results of the low temperature monochromatic transmission as a function of magnetic field obtained by the short pulse technique. **D)** Fan chart of $MAPbI_3$ for the small grain polycrystalline sample. The circular data points are from long pulse field measurements and star symbol points are collected by short pulse mega-gauss measurements. The solid lines and the dashed lines are the fits to the set of Landau levels and the excitonic transitions, respectively.

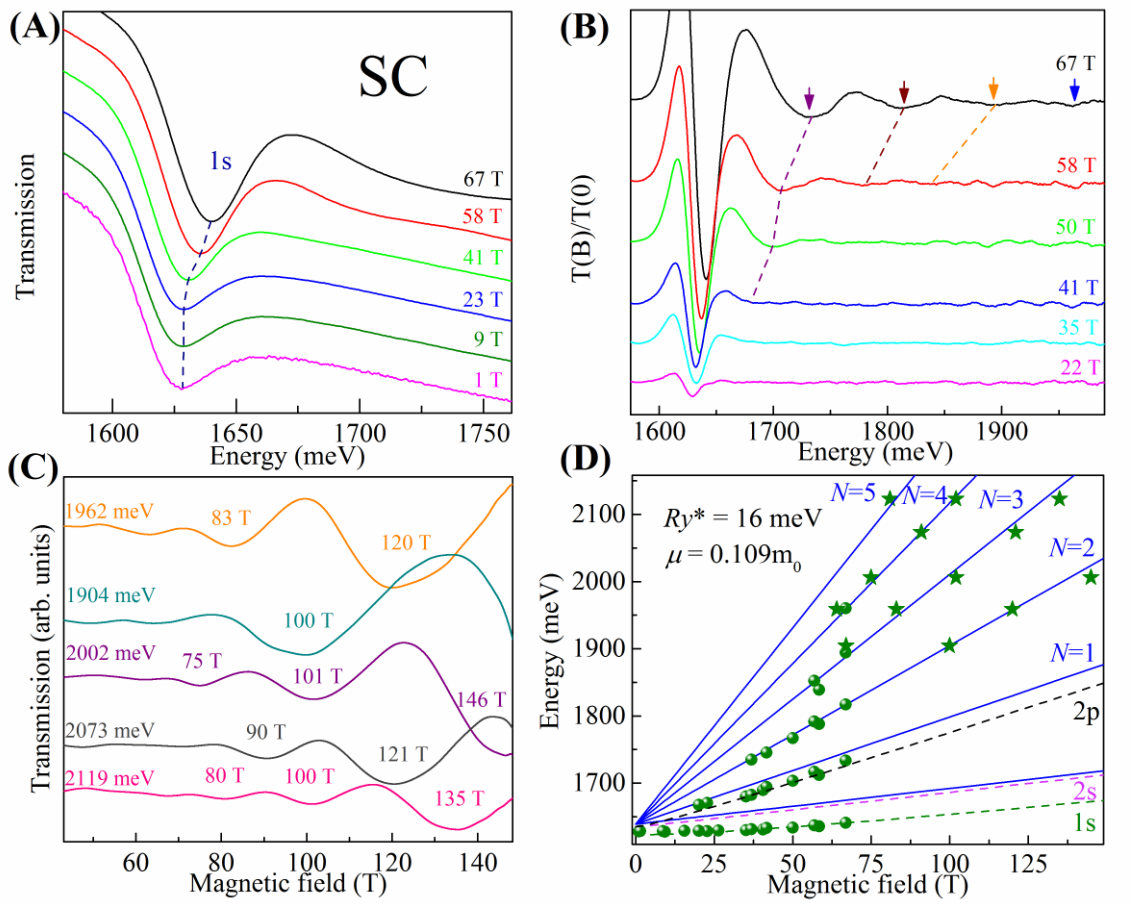

Figure S2 Magneto-optical transmission spectrum and fan chart measured at 2 K. A) Sequence of typical optical transmission spectra of the **SC** sample measured at the indicated magnetic fields which show the 1s excitonic transition with increased transmission. **B)** Sequences of the ratios of the transmission spectra in magnetic field $T(B)$ to that measured at zero field $T(0)$. The resonant absorption features of the free carrier Landau levels correspond to minima. **C)** Typical results of the low temperature monochromatic transmission as a function of magnetic field obtained by the short pulse technique. **D)** Fan chart of $MAPbI_3$ for the small grain (SC) sample. The circular data points are from long pulse field measurements and star symbol points are collected by short pulse mega-gauss measurements. The solid lines and the dashed lines are the fits to the set of Landau levels and the excitonic transitions, respectively.

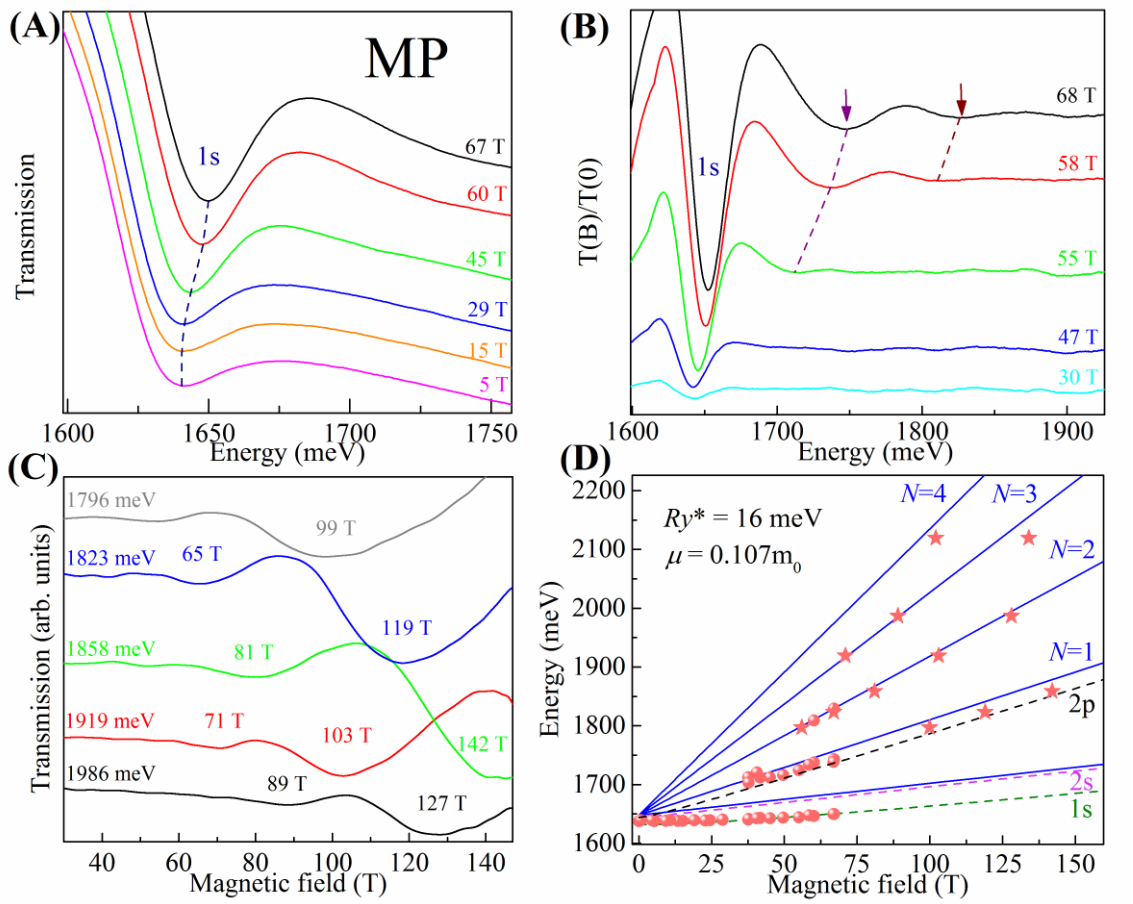

Figure S3 Magneto-optical transmission spectrum and fan chart measured at 2 K. A) Sequence of typical optical transmission spectra of the **MP** sample measured at the indicated magnetic fields which show the 1s excitonic transition with increased transmission. **B)** Sequences of the ratios of the transmission spectra in magnetic field $T(B)$ to that measured at zero field $T(0)$. The resonant absorption features of the free carrier Landau levels correspond to minima. **C)** Typical results of the low temperature monochromatic transmission as a function of magnetic field obtained by the short pulse technique. **D)** Fan chart of $MAPbI_3$ for the mesoporous small grain (MP) sample. The circular data points are from long pulse field measurements and star symbol points are collected by short pulse mega-gauss measurements. The solid lines and the dashed lines are the fits to the set of Landau levels and the excitonic transitions, respectively.

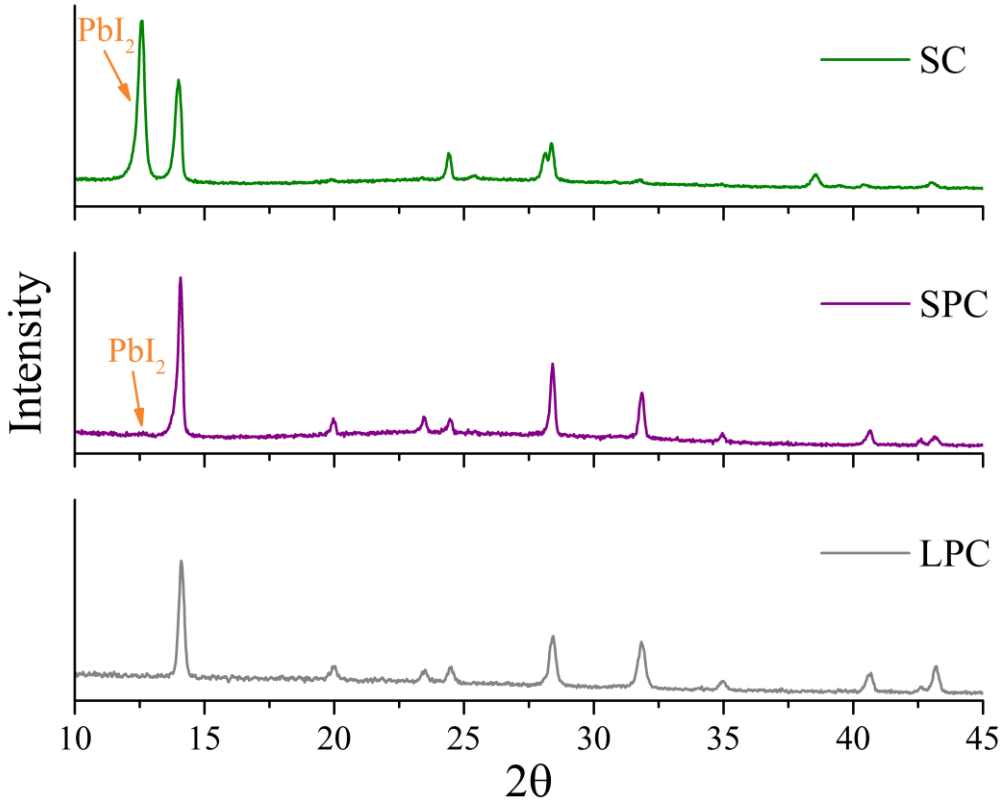

Figure S4 X-Ray Diffraction (XRD) patterns of different $MAPbI_3$ microstructures.

The XRD patterns show that the LPC, SPC and SC $MAPbI_3$ thin films exhibit the tetragonal perovskite structure. There exists small amount of crystalline PbI_2 impurities in the SPC and SC samples (see the features at an angle of 12.5º), indicating that the presence of small amounts of PbI_2 seemingly does not affect the excitonic properties of perovskites.

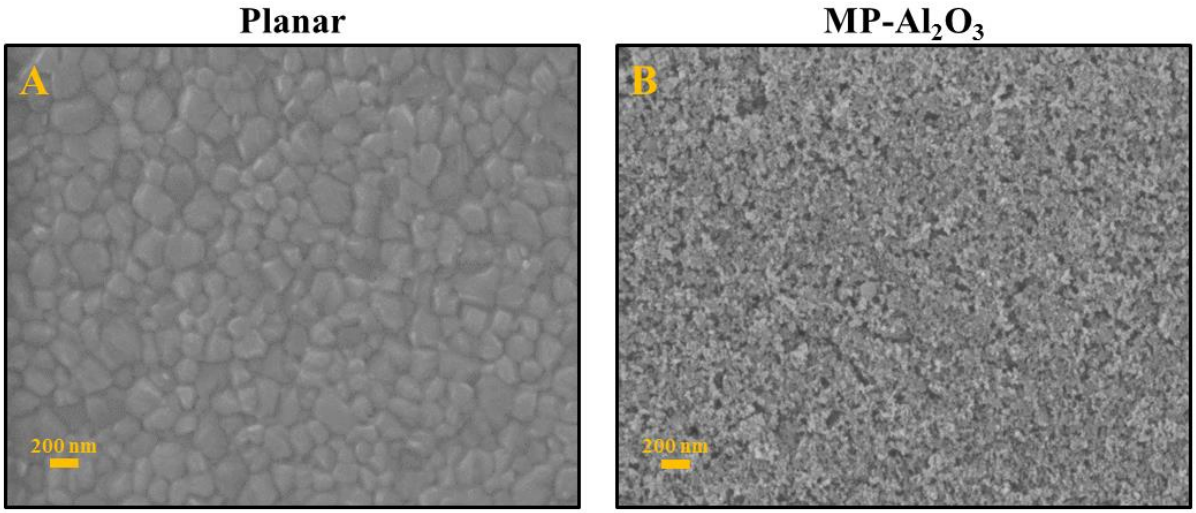

Figure S5 Morphology of $Cs_{0.05}(MA_{0.17}FA_{0.83})_{0.95}Pb(I_{0.83}Br_{0.17})_3$ samples. Top-view SEM images of the triple-cation lead mixed-halide layer with two different morphologies fabricated on glass substrates. **A)** Polycrystalline planar thin film. **B)** $Cs_{0.05}(MA_{0.17}FA_{0.83})_{0.95}Pb(I_{0.83}Br_{0.17})_3$ infiltrated into a thick mesoporous-Al_2O_3 (MP-Al_2O_3) scaffold. Scale bars are 200 nm.

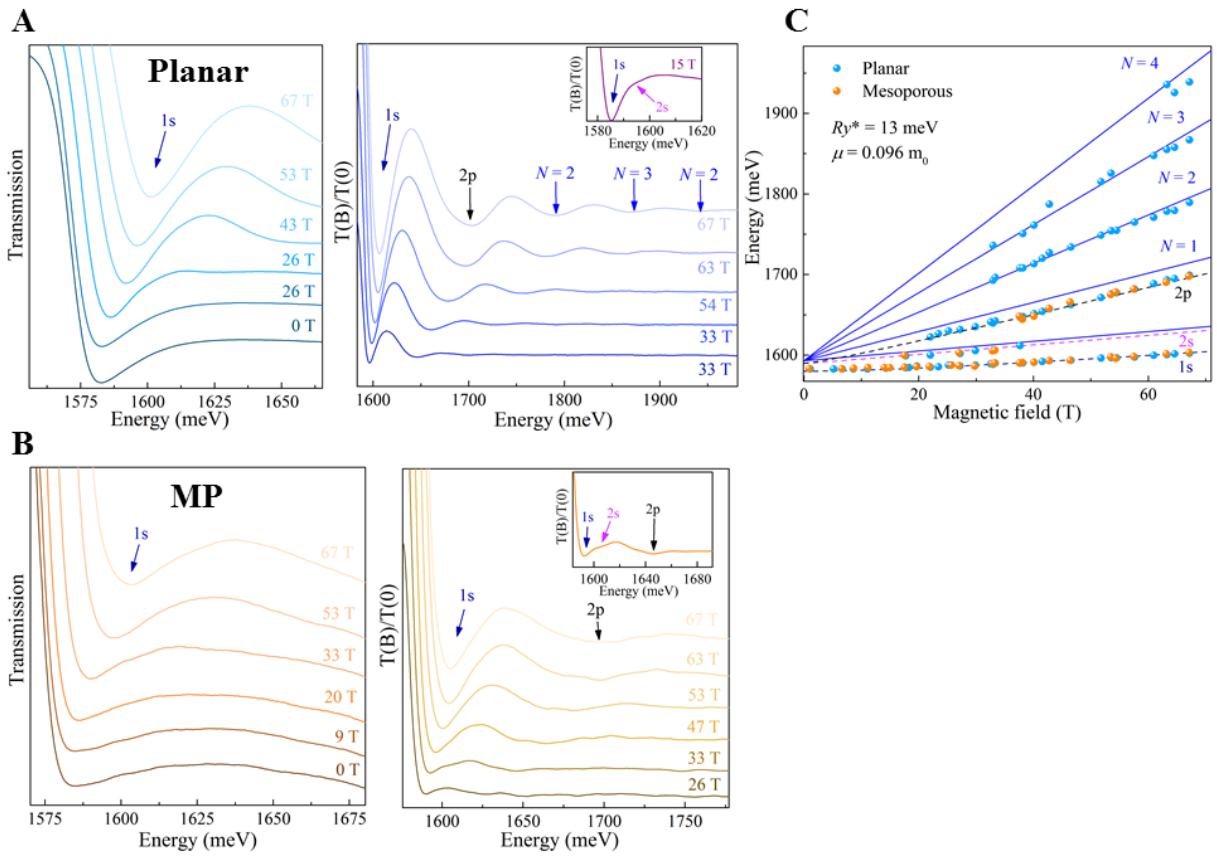

Figure S6 Magneto-optical transmission spectra and fan chart of $Cs_{0.05}(MA_{0.17}FA_{0.83})_{0.95}Pb(I_{0.83}Br_{0.17})_3$ measured at 2 K. A and B) Left panels: sequence of typical optical transmission spectra of the planar polycrystalline (A) and perovskite-infiltrated mesoporous-Al_2O_3 (B) samples measured at the indicated magnetic fields which show the 1s excitonic transitions with increased transmission. **A and B)** Right panels: sequences of the ratios of the transmission spectra in magnetic field $T(B)$ to that measured at zero field $T(0)$ for both triple-cation lead mixed-halide samples. **C)** Overlaid fan chart of the Planar and MP samples. The solid lines and the dashed lines are the fits to the set of Landau levels and the excitonic transitions, respectively.

Table S1 Summary of the parameters of the fits to the fan chart for the two different morphologies of $Cs_{0.05}(MA_{0.17}FA_{0.83})_{0.95}Pb(I_{0.83}Br_{0.17})_3$ in the low temperature (2 K), orthorhombic phases. The figures in the brackets are the error estimates of the parameters.

	E_g (meV)	μ (m_0)	Ry^* (meV)
Planar	1593(2)	0.096(0.002)	13(2)
Mesoporous	1594(2)	0.096(0.008)	13(2)

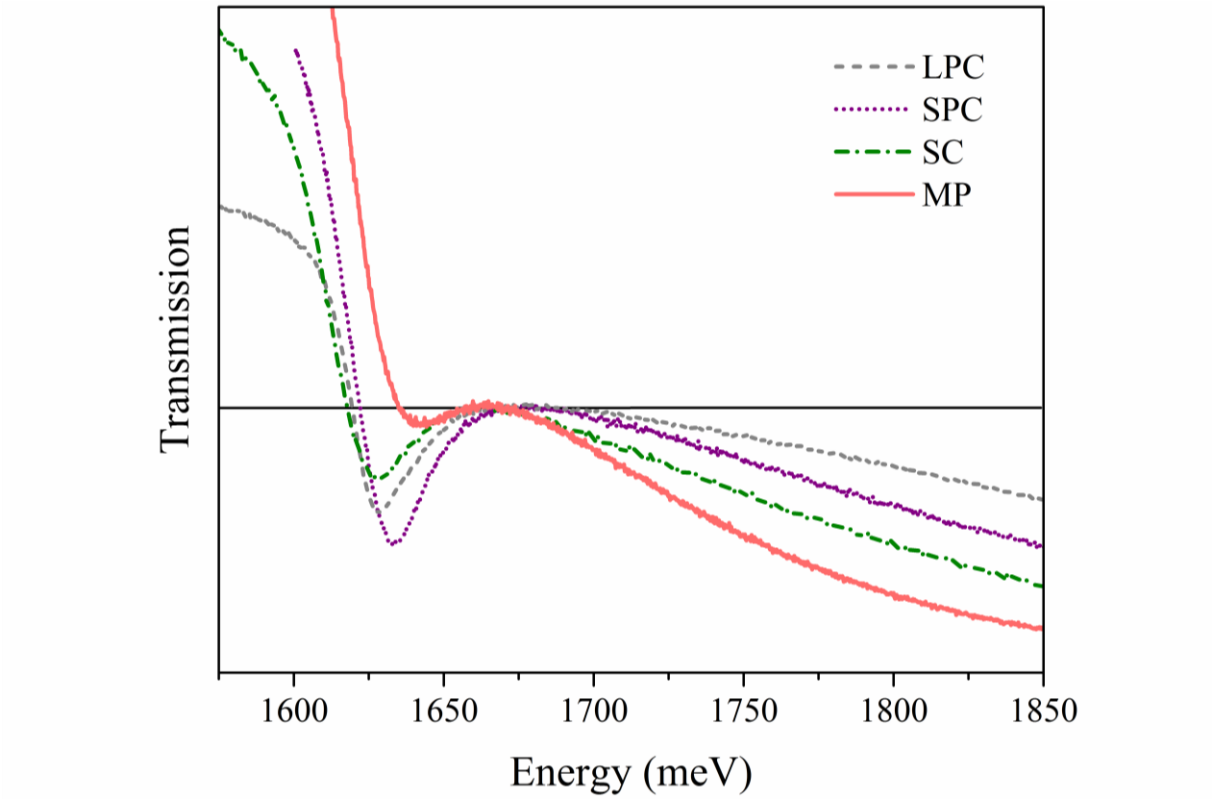

Figure S7 Transmission spectra of four different $MAPbI_3$ morphologies. The transmission spectra of **MP** (solid line), **SC** (dash-dotted line), **SPC** (dotted line) and **LPC** (dashed line) samples are normalized to a point on the plateau at the higher energy end of their spectrum.

These transmission results show different excitonic transition strength (corresponding to a dip in transmission spectra) at the absorption edge while the excitonic binding energy and effective mass remained relatively unchanged in these various microstructures (see panel C of Figure 3 and Table 1 in the main text).